Amino Acids (2006) 31: 309–316
DOI 10.1007/s00726-006-0365-3

Amino Acids
Printed in Austria

$p21^{WAF1/CIP1}$ and 14-3-3 σ gene expression in degenerated aortic valves: A link between cell cycle checkpoints and calcification

O. Golubnitschaja[1], **K. Yeghiazaryan**[1], **D. Skowasch**[2], **H. Schild**[1], and **G. Bauriedel**[2]

[1] Department of Radiology, Rheinische Friedrich-Wilhelms-University of Bonn, Bonn, Germany
[2] Department of Cardiology, Rheinische Friedrich-Wilhelms-University of Bonn, Bonn, Germany

Received February 24, 2006
Accepted April 20, 2006
Published online September 5, 2006;

Summary. The mechanisms underlying aortic valve degeneration are largely unknown. Cardiac tissue responds to a variety of stimuli by hypertrophic growth. Molecular mechanisms resulting in the hypertrophic response indicate similarity and overlap with those involved in both cell growth and death. We hypothesized cell cycle control to be the key event in progression regulation of heart valve degeneration followed by tissue mineralization. Human post-operative tissue samples of native non-rheumatic stenosed aortic valves were categorized according to absence (group 1) or presence of calcification (group 2). The samples were ex vivo examined for cell density and presence of macrophage (CD68), as well as expression of two checkpoint genes, $p21^{WAF1/CIP1}$ and 14-3-3 σ, arresting the G_1 and G_2 cell cycle phases, respectively. Expression rates were measured by "Real-Time"-PCR on transcriptional level. Target protein expression was measured and their co-localization in different kinds of valvular cells was tested using immunohistochemical analysis. Whereas macrophages were localized predominantly in sub-endothelial layer of valvular fibrosis, $p21^{WAF1/CIP1}$ and 14-3-3 σ expression was observed also in the valvular spongiosa co-localized with alpha-actin positive cells. Significantly higher cell density and inflammation grade were observed in group 2 versus group 1. Accordingly, $p21^{WAF1/CIP1}$ and 14-3-3 σ expression was several fold higher in group 1 versus group 2 on both transcription and translation levels. The present findings on degenerated aortic valves show that increased cell density accompanied with consequent calcification might be attributed to the down-regulation of both G_1 and G_2 checkpoint genes.

Keywords: Aortic valve degeneration – Calcification – Valvular fibrosis and spongiosa – Cell density and inflammation grade – Molecular monitoring ex vivo – Cell cycle checkpoints

Introduction

Pathomechanisms leading to the calcification of heart valves are still unclear. Cuspal calcific deposits in the heart are non-physiologic and normally not found in healthy cardiovascular tissues, but their deposition is usual for the physiological formation of bones (Bostrom et al., 1993; Kim, 1995; Srivatsa et al., 1997; Cipollone et al., 2001; Jian et al., 2001). Numerous clinical-pathological studies of calcified valves have demonstrated cuspal calcific deposits to be associated with mineralization of devitalized cells in native valves (Srivatsa et al., 1997) indicating the programmed molecular events in myocardial cells associated with their degeneration. Although cardiac cells undergo terminal differentiation soon after birth, irreversibly withdrawing from the cell cycle, growth stimulation induces cell hypertrophy, the first visible step of a developing imbalance in the maintenance of the cardiac cell population. This hypertrophic growth has been shown to be associated with the re-activation of the fetal gene program in cardiac cells (Liu and Olson, 2002; Bär et al., 2003), the clue of which is the positive regulation of the cell cycle progression. This switch in program might be crucial for the myocardial cell regulation. Such growth stimulation is responsible for up-regulated activity of cyclin-dependent kinases (CDKs) that consist of a kinase core and an associated cyclin subunit acting as the positive regulator (Sherr, 1994). Thereby different CDK inhibitors keep the negative control over CDKs activities.

CDK inhibitors are classified on the basis of their sequence homology and substrate specificity. Recently a novel cardiac helicase CHAMP that inhibits cell proliferation and cardiac hypertrophy was described (Liu and Olson, 2002). The CHAMP-dependent inhibition of cardiac hypertrophy is accompanied by an obligatory up-regulation of the cyclin-dependent protein-kinase inhibitor $p21^{WAF1/CIP1}$, a 21-kDa protein, which is a member of the CIP/KIP family (Sherr, 1994). Furthermore, a targeted

over-expression of $p21^{WAF1/CIP1}$ prevents cell enlargement and suppresses a specific gene expression of the cardiac hypertrophy markers in the cell population in vitro (Tamamori et al., 1998) indicating the key role of $p21^{WAF1/CIP1}$ in the regulation of the hypertrophic response.

Checkpoint function in the G_2 phase of the cell cycle before initiation of mitosis has 14-3-3 σ gene (Samuel et al., 2001). The important role of both $p21^{WAF1/CIP1}$ and 14-3-3 σ in the regulation of cardiac cell population under stress conditions has been demonstrated using the rat model of taurine depletion associated with oxidative stress, significant DNA-damage in cardiac cells, and the development of cardiomyopathy (Golubnitschaja et al., 2003). Since both $p21^{WAF1/CIP1}$ and 14-3-3 σ genes control the transition between proliferation and degradation of cardiac cells, we hypothesized here that a possible reduction in the expression rate of both genes might be associated with an increased density of damaged cell population followed by devitalization of cardiac tissue with a consequent remodeling of heart valves. Therefore, this ex vivo study examined relative cell density, inflammation grade, and expression levels of both checkpoint factors in non-calcified (group 1) versus calcified (group 2) human degenerated aortic valves in order to estimate the impact of these factors in molecular mechanisms of developing calcification.

Methods

Characterization of patients and collection of aortic valve samples

The diagnosis of non-rheumatic aortic valve stenosis was based on detailed history, physical examination of the patients, corresponding echocardiographic and other routine findings. Immediately after the tissue collection, an aliquot of each extracted aortic valve tissue has been shock frozen in liquid nitrogen and stored at −80 °C for further RNA and protein analysis, as well as cell density determination, and macrophage detection. The investigation conforms with the principles outlined in the Declaration of Helsinki and was performed with permission from the Ethics Committee of Medical Faculty, University of Bonn.

Assessment of cell density

Morphometric assessment of cell density in intimal regions was performed by counting hematoxylin-stained cell nuclei on a high-resolution video monitor (Endovision 534, Storz Inc., Germany). The microscopic image (Optiphot-2, Nikon, Germany) was relayed by a miniaturized video camera (Endovision 534) to a downstream monitor (final magnification, ×500). Ten randomly selected tissue areas, each encompassing 0.4 mm^2, were assessed per each sample, and the corresponding number of cells was counted. Morphometric examination of cell density was performed by two independent investigators in a double-blind fashion.

Assessment of macrophages tissue detection

Monoclonal antibodies specific for macrophages (CD68) were obtained from Boehringer Inc. (Germany). The color reaction was done with APAAP marking (Dako, Denmark) according to a standard protocol. Positive immunohistochemical reaction was marked by distinct, red to lilac signals. Nuclear counter-staining was performed by standard hematoxylin staining. Histological sections were photographed by a Nikon Optiphot-2-photomicroscope (Nikon, Germany) using Kodak Ektachrome 100 ISO color films.

Isolation of total RNA and mRNA

Total RNA was extracted using the commercial RNAzol-B isolation kit (WAK-Chemie Medical GmbH, Germany), and an isolation of mRNA from the individual total RNA-pools was performed using the Oligotex® mRNA Mini Kit (Qiagen, Germany) according to protocols supplied by the manufactures.

Reverse transcriptase PCR (RT-PCR) and "real-time"-quantitative PCR (RT-QPCR)

In order to detect the expression of target genes qualitatively and to optimize individual reaction conditions for concomitant "real-time"-quantitative PCR, reverse-transcriptase PCR has been performed using specific primer-sets designed to β-actin (accession number BC014861, positions 203–221 and 411–394 bp in cDNA), $p21^{WAF1/CIP1}$ (accession number Z85996, positions 8605–8622 bp in exon 2 and 10271–10254 bp in exon 3 of chromosomal DNA), and 14-3-3 σ (accession number AF029082, positions 56–75 and 334–315 bp in cDNA). Synthesized oligonucleotides had following sequences: for β-actin – 5′GATGGTGGGCA TGGGTCAG3′ and 5′TGGGGTTCAGGGGGGCCT3′, for $p21^{WAF1/CIP1}$ – 5′CAGAACCGGCTGGGGAT3′ and 5′CGGCGTTTGGAGTGGTAG3′, and for 14-3-3 σ – 5′GTGTGTCCCCAGAGCCATGG3′ and 5′ACCTTC TCCCGGTACTCACG3′ used as forward and reverse primers respectively. cDNA synthesis was performed using the "First-Strand cDNA Synthesis Kit" (GE Healthcare, UK). For each cDNA synthesis, 1 μg mRNA was reverse transcribed using the oligo(dT)18 primer in a final volume of 33 μl each, according to the protocol supplied by the manufacturer. After heat inactivation of reverse transcriptase 2 μl of the cDNA were used for each PCR amplification. The PCR mixture contained 1 × PCR buffer (16.6 mM ammonium sulfate, 67 mM Tris, pH 8.8, 6.7 mM $MgCl_2$, 10 mM 2-mercaptoethanol), dNTPs (each at 1.25 mM), primer pairs (100 pM each per reaction), and cDNA-template in a final volume of 50 μl. Reactions were started at 95 °C for 5 min before adding 1.5 units of Taq Polymerase (Red-Hot®, ABgene, UK) at the annealing temperature of 56 °C followed by the polymerization at 72 °C for 1 min. Amplification was carried out in a Perkin Elmer "DNA Thermal Cycler TC480" for 45 cycles (denaturation for 45 sec at 95 °C, annealing for 45 sec at 56 °C, and polymerization at 72 °C for 30 sec), followed by a final 7 min extension at 72 °C. Negative controls without DNA as well as positive controls with a sequenced template were performed for each set of PCR experiments. PCR products (50 μl) were directly loaded onto 3% agarose gels ("Wide Range"-Agarose for analysis of DNA fragments longer than 50 bp, Sigma-Aldrich, UK), stained with ethidium bromide after electrophoresis, and directly visualized under UV illumination. The specificity of the amplification was controlled for each PCR product using site specific restriction analysis.

For the quantitative profiling of the target gene expression RT-QPCR has been used. SYBR® Green I was utilized as the intercalation dye and fluorescent reporter molecule detecting the accumulation of the amplified double-stranded product in the iCycler iQIM Detection System (Bio-Rad, USA) according to the protocol supplied by manufacturer. An aliquot of 2 μl of the synthesized cDNAs has been used for each RT-QPCR analysis. The reaction mixtures had the same contents as for RT-PCR with an exception of Red-Hot® polymerase (ABgene, UK) which has been substituted for "Thermoprime Plus DNA Polymerase" from ABgene (UK) in order to avoid color signal disturbances. The same optimized amplification program described above has been also for quantitative real-time PCR analysis. The algorithm of the iCycler iQIM Detection System normalizes the reporter signal (non-intercalated SYBR® Green I) to a passive refer-

ence and multiplies the SD of the background signal in the first few cycles by a default factor of 10, to determine a threshold (Heid et al., 1996). By subtracting the difference of the C_t values of the gene of interest from those of the housekeeping gene (β-actin), the data have been normalized. Relative levels were calculated for gene expression in group 2 versus group 1 based on the differences in C_t values.

The specificity of PCR amplification was controlled using the site specific restriction analysis of target PCR products. The amplification products underwent an extraction from the agarose gel using DNA isolation kit (Hybaid-AGS GmbH, Germany) before digestion. They were digested in a final volume of 50 µl with 20 units of each restriction endonuclease for 2 h, according to conditions specified by the manufacturer (Fermentas, Lithuania).

Localization of $p21^{WAF1/CIP1}$ and 14-3-3 σ protein expression in valvular tissue

Polyclonal antibodies specific for $p21^{WAF1/CIP1}$ and 14-3-3 σ were obtained from Santa Cruz (USA). Monoclonal antibodies specific for alpha-actin were obtained from Boehringer Inc. (Germany). Each immunohistochemical reaction was done with APAAP marking (Dako, Denmark) according to a standard protocol. A localization and co-localization of all three proteins in the tissue was monitored. Histological sections were photographed by a Nikon Optiphot-2-photomicroscope (Nikon, Germany) using Kodak Ektachrome 100 ISO color films.

Results

Patients data

Demographic data of all patients are provided in Table 1. Some of the patients underwent surgery because of isolated valve stenosis, while others with milder valvular degeneration underwent a combined procedure, usually including coronary bypass grafting. This enabled us to obtain a relatively comprehensive range of disease conditions. According to their calcification severity grade, the extracted tissue samples were classified as non-calcified (opaque leaflet with focal areas of thickening and stiffness, group 1 with 7 samples) or calcified (definite areas of calcification, prominent cusp thickening, group 2 with 5 samples). In 3 cases, valvular tissue was divided between groups 1 and 2 due to different local calcification grades (numbers 1 and 6, 3 and 8, as well as 4 and 10 as demonstrated in Table 1).

Macrophage content and cellular density

Macrophages detected by CD68 immunostaining were observed in serial sections of each degenerated aortic valve and was predominantly confined to valvular fibrosa. Representative examples of degenerated aortic valves that demonstrate clusters of macrophages are illustrated for both non-calcified and calcified tissue in Fig. 1Aa and Ab, respectively. Morphometric immunohistochemical evaluations demonstrated a considerably varying cellular density (between 500 and 4000 cells/mm^2) and degree of macrophage signaling (0 to 14% of total cell number) among the valvular tissue samples tested. When aortic valve specimens were macroscopically categorized into groups 1 and 2, significantly higher cellular density and more frequent appearance of macrophages were found in the latter compared to the first group. The results are shown in Fig. 1B and C respectively. Although the number of detected macrophages varied considerably in each group, however, no correlation between tissue cell density and frequency of macrophage appearance could be found. Moreover, whereas no correlation between inflammatory and calcification grade was found, an increased cell density over 1700 cells/mm^2, in contrast, was found to be characteristic for the calcification (Table 1).

Table 1. Characteristics of patients (n = 9) and lesions (n = 12)

Valve no.	Group	Age/ gender	CHD y/n	Risk factors	Medication	CD68 expression, %	Cellular density, cells/mm^2
1	2	76/F	y	H, A, L	ace, diu	7.2	1775
2	2	52/F	n	H	beta, diu	4.5	4041
3	2	70/F	n	H, A, L	ace, diu, dig, cou	5.9	2696
4	2	82/M	y	H, A, L	diu, asa, sta, ace	14.3	2537
5	2	52/F	n	H	beta, diu	3.6	2288
6	1	76/F	y	H, A, L	ace, diu, cou	1.6	876
7	1	71/F	n	N, L	asa	1.0	794
8	1	70/F	n	H, A, L	ace, dig, diu, cou	0.8	569
9	1	75/M	y	H	dig, asa, ace, sta, diu, beta, cou	9.6	600
10	1	82/M	y	H, A, L	asa, diu, sta, ace	10.2	1669
11	1	74/F	y	L, H	asa, ace, dig	0	535
12	1	54/M	y	H	sta, cou	4.1	1121

H Hypertension, *L* hyperlipidemia, *A* adipositas, *N* nicotine, *asa* acetyl salicylic acid, *cou* coumadine, *sta* statin, *ace* ace inhibitor, *diu* diuretics, *dig* digoxin/digitoxin, *beta* beta-blocker

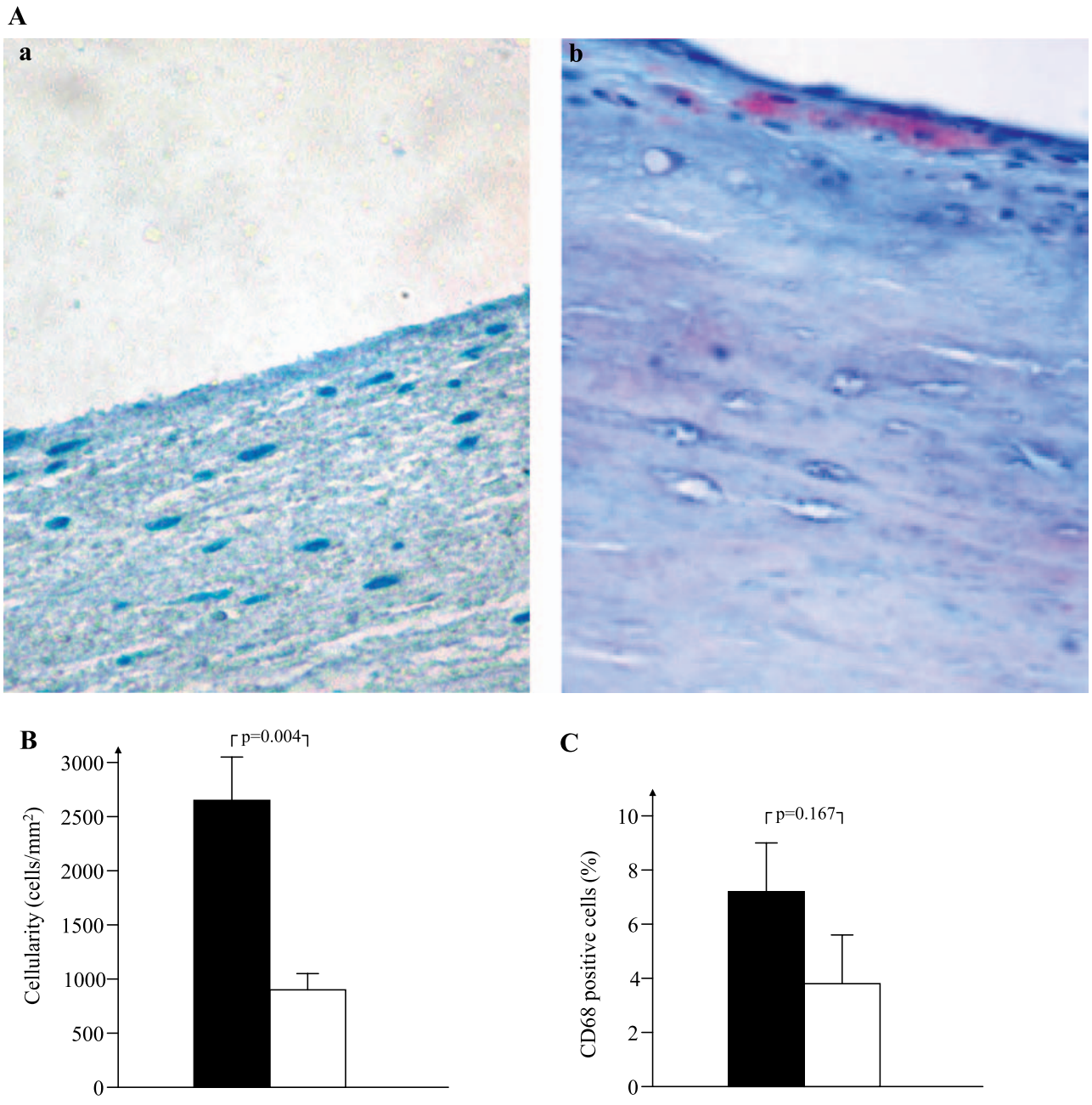

Fig. 1. Comparative immunohistochemical detection of macrophages and analysis of cell density in groups 1 and 2: **A** Detection of CD68 positive cells (macrophages) in a degenerated non-calcified (*a*) and calcified (*b*) aortic valves; note that macrophages are predominantly present in sub-endothelial lesions and are sparsely distributed in valvular spongiosa and ventricularis. **B** Bar graphs comparing cellular density in group 2 (■) versus group 1 (□) in degenerated aortic valves. Data are given in counted cells/mm^2 ± SEM. **C** Bar graphs comparing frequency of macrophages in group 2 (■) versus group 1 (□) in degenerated aortic valves. Data are given in CD68 positive cells in % ± SEM

Detection of target transcripts

RT-PCR revealed the house-keeping β-actin, $p21^{WAF1/CIP1}$ and 14-3-3 σ genes expressed in both calcified and non-calcified regions of aortic valves (Fig. 2A, B, and C, respectively). The amplification of each target PCR product was performed specifically as confirmed by restriction analysis based on the site-specific nuclease cleavage of target DNA fragments (Fig. 3A, B, and C, respectively).

Quantification of target transcripts

The precise RT-QPCR quantitative analysis showed tissue specific expression patterns, which positively

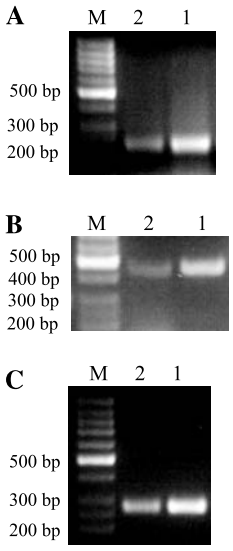

Fig. 2. Results of semi-qualitative RT-PCR analysis of gene expression in group 1 (*1*) and group 2 (*2*) valvular tissue; amplification products: **A** β-actin fragment (used as an internal standard) with an expected length of 209 bp. **B** $p21^{WAF1/CIP1}$ with an expected length of 460 bp. **C** 14-3-3 σ with an expected length of 279 bp; *M* 50 bp DNA ladder (GeneRuler™, Fermentas, Lithuania)

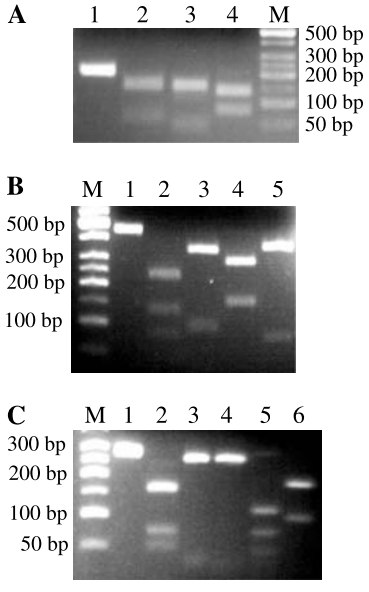

Fig. 3. Results of restriction analysis: **A** AluI to get 57 and 152 bp fragments, HaeIII to get 14, 45 and 150 bp fragments, RsaI to get 78 and 131 bp fragments from the 209 bp of β-actin amplification product, **B** AluI to get 84, 138 and 241 bp fragments, HhaI to get 105 and 358 bp fragments, PstI to get 158 and 305 bp fragments, PvuII to get 84 and 379 bp fragments from the 463 bp of $p21^{WAF1/CIP1}$ amplification product; **C** AluI to get 50, 72 and 157 bp fragments, ApaI to get 26 and 253 bp fragments, AvaI to get 27 and 252 bp fragments, HaeIII to get 18, 28, 45, 73 and 115 bp fragments, HhaI to get 102 and 177 bp fragments from the 279 bp of 14-3-3 σ amplification product

Table 2. Relative gene transcription of $p21^{WAF1/CIP1}$ and 14-3-3 σ calculated based on C_t values given as a mean from 2 parallel measurement by RT-QPCR; SD = standard deviation

Valve no.	$p21^{WAF1/CIP1}$ transcription relative to β-actin	14-3-3 σ transcription relative to β-actin
1	0.00074	0.00082
2	0.00006	0.00003
3	0.00023	0.00026
4	0.00035	0.00039
5	0.00048	0.00050
	Mean value ± SD in group 2: 0.00037 ± 0.00019	Mean value ± SD in group 2: 0.00040 ± 0.00023
6	3.0	2.5
7	3.8	3.4
8	4.3	3.3
9	4.1	4.1
10	1.8	1.2
11	4.9	4.3
12	2.6	1.0
	Mean value ± SD in group 1: 3.5 ± 0.9	Mean value ± SD in group 1: 2.7 ± 1.1

correlated with the calcification appearance in all samples examined: expression of $p21^{WAF1/CIP1}$ was about 10,000 fold higher in group 1 compared to group 2. Likewise, the expression rates of 14-3-3 σ were about 13,000 fold higher in group 1 compared to group 2 (Table 2).

Localization and quantification of $p21^{WAF1/CIP1}$ and 14-3-3 σ protein expression

The results of immunohistochemical analysis of $p21^{WAF1/CIP1}$ and 14-3-3 σ protein expression rates correlated well with those measured on the level of transcription using RT-QPCR (Tables 2 and 3). Thereby, no target protein expression could be detected in tissue samples of group 2. In contrast, the expression of 14-3-3 σ and $p21^{WAF1/CIP1}$ was observed in both subendothelial layer and valvular interstitium of tissue samples in group 1. Moreover, being overall distributed in the valvular tissue, this protein expression, however, was mainly co-localized with alpha-actin in the valvular spongiosa.

Correlation coefficients calculated for the relative protein expression in relationship to the cell density (Table 4) clearly demonstrated a significant down-regulation of both genes with increasing cell density in group 2 compared to group 1.

Table 3. Evaluation of protein expression levels as well as co-localization of 14-3-3 σ, $P21^{WAF1/CIP1}$, and alpha-actin in tissue samples as shown by immunohistochemical analysis

Valve no.	Group	Cellular density, cells/mm^2	CD68, %	14-3-3 σ, relative units	$P21^{WAF1/CIP1}$, relative units	Alpha-actin, relative units
1	2	1775	7.2	0.0	0.0	23.9
2	2	4041	4.5	0.0	0.0	11.3
3	2	2696	5.9	0.0	0.0	34.9
4	2	2537	14.3	0.0	0.0	32.8
5	2	2288	3.6	0.0	0.0	72.2
6	1	876	1.6	18.9	13.9	62.8
7	1	794	1.0	7.9	18.6	34.3
8	1	569	0.8	7.7	14.9	58.4
9	1	600	9.6	14.7	24.8	43.6
10	1	1669	10.2	21.2	14.3	33.8
11	1	535	0.0	12.5	11.9	15.3
12	1	1121	4.1	20.9	16.2	35.4

Table 4. Correlation coefficients for the target expression rates on the level of transcription and translation to both cell density and macrophage content calculated as a ratio of mean values in groups 1 and 2

Group	Relative transcription rates/cell density for		Relative protein rates/cell density for		Relative transcription rates/macrophage content for		Relative protein rates/macrophage content for	
	$p21^{WAF1/CIP1}$	14-3-3 σ	$p21^{WAF1/CIP1}$	14-3-3 σ	$p21^{WAF1/CIP1}$	14-3-3 σ	$p21^{WAF1/CIP1}$	14-3-3 σ
1	4.0×10^{-3}	3.1×10^{-3}	1.9×10^{-2}	1.7×10^{-2}	9.0×10^{-1}	6.9×10^{-1}	4.2	3.8
2	1.0×10^{-7}	1.0×10^{-7}	0.0	2.0×10^{-4}	5.2×10^{-5}	5.6×10^{-5}	0.0	7.6×10^{-2}

Discussion

In contrast to the genetically programmed and physiologically well regulated mineralization of skeletal and dental tissue, non-physiologic calcification occurs in numerous pathologic cardiovascular conditions including atherosclerosis, valvular stenosis, and reperfused ischemic myocardium. This is proposed to be an undesired but common feature of degenerative or/and inflammatory tissue changes throughout the body. Both degenerative and inflammatory tissue remodeling modulates the tissue homeostasis, which depends on the balance of cell growth and death. Thereby, a proper regulation of cell cycle seems to be crucial for the maintenance of a physiological cell population. Molecular mechanisms underlying a cardiac tissue resistance towards degenerative tissue remodeling followed by aortic valve calcification are largely unknown. Here we report our very recent experimental data, which indicate a clear correlation among

- the well coordinated regulation of checkpoint genes arresting cell cycle in G_1 and G_2 phases,
- modulation of the density of valvular cell population, and
- progressive calcification of native aortic valve tissue.

Cell cycle control obviously plays a key role in the maintenance of cardiac cell population: high rates of cell death have been shown to be physiological in normal adult human hearts and those of mice and rats (Nadal-Ginard, 2001). The physiological expression of $p21^{WAF1/CIP1}$ shows a gradual increase during development in both rat and man, becoming maximal in adulthood (Burton et al., 1999). A direct link between the Bcl-2 dependent down-regulation of $p21^{WAF1/CIP1}$ and an increased myocyte density in the left ventricle has been shown recently in experimental work with transgenic mice (Limana et al., 2002). These findings are in agreement with our results which clearly demonstrate that down-regulation of both checkpoint genes correlates with increasing cardiac cell density and calcification appearance in aortic valve tissue. This work is the first report about the co-ordinate regulation of both G_1 and G_2 checkpoints in degenerative valves. The validation of target gene products was done on both transcriptional and translational levels. The measurement at the transcriptional level was performed using the most sensitive quantification method of "real-time"-quantitative PCR. Expressional levels measured in calcified tissue samples (group 2) were extremely low compared

to those in non-calcified tissue (group 1). The corresponding normalized C_t values in group 2 were almost identical for both $p21^{WAF1/CIP1}$ and 14-3-3 σ genes, and showed, therefore, the coordinated suppression of both checkpoints in at calcification. Additionally, immunohistochemical analysis of the target protein expression shows a clear correlation between transcription and translation levels of the target gene products: whereas no specific signals were monitored in the calcified tissue, the target proteins appeared in both the sub-endothelial layer of the valvular fibrosa and valvular interstitium of non-calcified tissue. Whereas CD68 positive signals, i.e. macrophages were localized predominantly in the sub-endothelial layer of the valvular fibrosa, 14-3-3 σ and $p21^{WAF1/CIP1}$ were observed in both sub-endothelial layer and valvular interstitium but mainly co-localized with alpha-actin in the valvular spongiosa, pointing the target expression predominantly in myofibroblasts. There is a growing body of evidence, however, that in response to stimulus/injury the heart valves undergo tissue remodeling including phenotypic modulation and transformation of fibroblast-like into myofibroblast-like cells (Schoen, 2005). Therefore, the target protein expression we observed in degenerated valvular tissue, can originate predominantly from myofibroblasts.

Correlation coefficients calculated for the mean values of the target protein expression indicate the clear functional link between the down-regulation of both checkpoint genes and growing cell density. Interestingly, the number of macrophages does not correlate with the cell density, whereas both the increased cell density and well coordinated down-regulation of $p21^{WAF1/CIP1}$ and 14-3-3 σ gene expression were found to be characteristic for calcification. Therefore, the coordinated double control over DNA quality/synthesis and cell proliferation in valvular cells might be efficient only in non-calcified tissue, whereas in the calcified one this control becomes coordinately suppressed in both G_1 and G_2 dependent checkpoints. These findings give further evidence that the efficiency of cell cycle control in human non-calcified valvular tissue depends not only on the positive/negative CDKs regulation in the G_1 phase but also on the coordinated regulation of both G_1 and G_2 dependent checkpoints, that has not been considered from the view point of molecular mechanisms until now. Recent in vitro experiments on rat cardiac fibroblasts showed, that a target up-regulation of inhibitors for G_1 dependent CDKs effectively suppresses the DNA synthesis and may decrease a potential risk of cardiovascular diseases (Mercier et al., 2002).

The dissociation of $p21^{WAF1/CIP1}$ from the CDK complexes correlates well with the activation of CDK2, CDK4, CDK6, and the release from cell cycle arrest, whereby the number of cardiac cells in S phase rises considerably (von Harsdorf et al., 1999). Further, in contrast to P16 (a specific inhibitor of CDK4/6), the ''universal'' CDKs inhibitor $p21^{WAF1/CIP1}$ was shown to be able to block completely an E2F-1-induced G_1 exit (Akli et al., 1999). However, E1A binding activity to target protein complexes has effects on the cell cycle progression beyond those produced by E2F-1 alone and can drive S-phase entry that is resistant to $p21^{WAF1/CIP1}$ (von Harsdorf et al., 1999). These facts explain the necessity of the coordinated regulation of both G_1 and G_2 dependent checkpoints, found in our work, in order to keep the control over the cell population maintenance in cardiac tissue. Noteworthy, from both relatively high expressed checkpoint genes in the non-calcified tissue, the expression of $p21^{WAF1/CIP1}$ was slightly higher than that of 14-3-3 σ. This asymmetric up-regulation in contrast to the well-balanced down-regulation of both genes in the calcified tissue indicates a differential necessity in the expression of these genes depending on the physiologic status of the valvular cell population.

Concluding remarks

Pronounced up-regulation of both genes in non-calcified in contrast to their down-regulation in calcified degenerated valvular tissue indicates the important role of checkpoint proteins in mechanisms keeping valvular cells alive and functional. Blockade of cell cycle progression results in a prolonged resistance to macrophage invasion and foam cell deposition (Mann et al., 1997). Therefore, it is likely that reduced cell cycle control in valvular tissue leads to the increased macrophage invasion that, in turn, can contribute to non-physiological calcification by both triggered unspecific inflammation and NO-toxicity (Schmidt and Walter, 1994; Zhuang and Wogan, 1997; Lutgens et al., 1999; Sanders et al., 2001; Frangogiannis et al., 2002). Taken together, our results demonstrate that the coordinated activation of both G_1 and G_2 dependent checkpoint genes may be an attribute of the valvular tissue resistance against the calcification processes. These data should be further taken into consideration, when designing therapeutic prevention towards pro-calcification molecular mechanisms in human hearts.

Acknowledgements

This research was supported by DFG (Deutsche Forschungsgemeinschaft, Germany) grant GO 978/4-1 to O.G. The authors thank Mrs. Nicole Kuhn and Mr. Hanno Schimikowski for their excellent technical assistance.

References

Akli S, Zhan S, Abdellatif M, Schneider MD (1999) E1A can provoke G1 exit that is refractory to p21 and independent of activating cdk2. Circ Res 85: 319–328

Bär MDH, Kreuzer J, Cojoc A, Jahn L (2003) Upregulation of embryonic transcription factors in right ventricular hypertrophy. Basic Res Cardiol 98: 285–294

Bostrom K, Watson KE, Horn S, Wortham C, Herman IM, Demer LL (1993) Bone morphogenetic protein expression in human atherosclerotic lesions. J Clin Invest 91: 1800–1809

Burton PB, Yacoub MH, Barton PJ (1999) Cyclin-dependent kinase inhibitor expression in human heart failure. A comparison with fetal development. Eur Heart J 20: 604–611

Cipollone F, Prontera C, Pini B, Marini M, Fazia M, De Cesare D, Iezzi A, Ucchino S, Boccoli G, Saba V, Chiarelli F, Cuccurullo F, Mezzetti A (2001) Overexpression of functionally coupled cyclooxygenase-2 and prostaglandin E synthase in symptomatic atherosclerotic plaques as a basis of prostaglandin E(2)-dependent plaque instability. Circulation 104: 921–927

Frangogiannis NG, Smith CW, Entman ML (2002) The inflammatory response in myocardial infarction. Cardiovasc Res 53: 31–47

Golubnitschaja O, Moenkemann H, Kim K, Mozaffari MS (2003) DNA damage and expression of checkpoint genes p21(WAF1/CIP1) and 14-3-3 sigma in taurine-deficient cardiomyocytes. Biochem Pharmacol 66: 511–517

Heid CA, Stevens J, Livak KJ, Williams PM (1996) Real time quantitative PCR. Genome Res 6: 986–994

Jian B, Jones PL, Li Q, Mohler ER 3rd, Schoen FJ, Levy RJ (2001) Matrix metalloproteinase-2 is associated with tenascin-C in calcific aortic stenosis. Am J Pathol 159: 321–327

Kim KM (1995) Apoptosis and calcification. Scanning Microsc 9: 1137–1178

Limana F, Urbanek K, Chimenti S, Quaini F, Leri A, Kajstura J, Nadal-Ginard B, Izumo S, Anversa P (2002) bcl-2 overexpression promotes myocyte proliferation. Proc Natl Acad Sci USA 99: 6257–6262

Liu ZP, Olson EN (2002) Suppression of proliferation and cardiomyocyte hypertrophy by CHAMP, a cardiac-specific RNA helicase. Proc Natl Acad Sci USA 99: 2043–2048

Lutgens E, de Muinck ED, Kitslaar PJ, Tordoir JH, Wellens HJ, Daemen MJ (1999) Biphasic pattern of cell turnover characterizes the progression from fatty streaks to ruptured human atherosclerotic plaques. Cardiovasc Res 41: 473–479

Mann MJ, Gibbons GH, Tsao PS, von der Leyen HE, Cooke JP, Buitrago R, Kernoff R, Dzau VJ (1997) Cell cycle inhibition preserves endothelial function in genetically engineered rabbit vein grafts. J Clin Invest 99: 1295–1301

Mercier I, Colombo F, Mader S, Calderone A (2002) Ovarian hormones induce TGF-beta(3) and fibronectin mRNAs but exhibit a disparate action on cardiac fibroblast proliferation. Cardiovasc Res 53: 728–739

Nadal-Ginard B (2001) Generation of new cardiomyocytes in the adult heart: prospects of myocardial regeneration as an alternative to cardiac transplantation. Rev Esp Cardiol 54: 543–550

Samuel T, Weber HO, Rauch P, Verdoodt B, Eppel JT, McShea A, Hermeking H, Funk JO (2001) The G2/M regulator 14-3-3 sigma prevents apoptosis through sequestration of Bax. J Biol Chem 276: 45201–45206

Sanders DB, Hunter K, Wu Y, Jablonowski C, Bahl JJ, Larson DF (2001) Modulation of the inflammatory response in the cardiomyocyte and macrophage. J Extra Corpor Technol 33: 167–174

Schmidt HH, Walter U (1994) NO at work. Cell 78: 919–925

Schoen FJ (2005) Cardiac valves and valvular pathology: update on function, disease, repair, and replacement. Cardiovasc Pathol 14: 189–194

Sherr CJ (1994) G1 phase progression: cycling on cue. Cell 79: 551–555

Srivatsa SS, Harrity PJ, Maercklein PB, Kleppe L, Veinot J, Edwards WD, Johnson CM, Fitzpatrick LA (1997) Increased cellular expression of matrix proteins that regulate mineralization is associated with calcification of native human and porcine xenograft bioprosthetic heart valves. J Clin Invest 99: 996–1009

Tamamori M, Ito H, Hiroe M, Terada Y, Marumo F, Ikeda MA (1998) Essential roles for G1 cyclin-dependent kinase activity in development of cardiomyocyte hypertrophy. Am J Physiol 275: H2036–H2040

von Harsdorf R, Hauck L, Mehrhof F, Wegenka U, Cardoso MC, Dietz R (1999) E2F-1 overexpression in cardiomyocytes induces downregulation of p21CIP1 and p27KIP1 and release of active cyclin-dependent kinases in the presence of insulin-like growth factor I. Circ Res 85: 128–136

Zhuang JC, Wogan GN (1997) Growth and viability of macrophages continuously stimulated to produce nitric oxide. Proc Natl Acad Sci USA 94: 11875–11880

Authors' address: O. Golubnitschaja, PhD, Prof. and Head of the Division of Molecular/Experimental Radiology, Department of Radiology, Rheinische Friedrich-Wilhelms-University of Bonn, Sigmund-Freud-Str. 25, D-53105 Bonn, Germany,

Fax: +49-228-287-4457, E-mail: Olga.Golubnitschaja@ukb.uni-bonn.de